Water-Augmented Turbofan Engine

W. Richard Davison* and Thomas J. Sadowski†
United Aircraft Research Laboratories, East Hartford, Conn.

This paper describes a novel lightweight propulsion scheme for use in high-speed ships in which large amounts of water are injected into the fan discharge duct of an aircraft-type turbofan engine. Theoretical design and off-design performance for this water-augmented turbofan engine show that dry thrust theoretically can be augmented 380% at 25 knots and 90% at 100 knots. The reduction in theoretical performance caused by nonoptimum rates of water injection and by two-phase flow losses is not sufficient to detract from significant thrust augmentation. The results show that in many marine vehicle applications the slightly lower propulsive efficiency of the water-augmented turbofan engine, relative to more conventional propulsion systems, is more than compensated for by its extremely low system weight.

Nomenclature

A = cross-sectional area for flow, ft²
C_p = heat capacity at constant pressure, Btu/lbm-°R
D_{po} = initial diameter of droplet, μ
F_{Net} = net specific thrust, lbf/lbm/sec of gas generator airflow
g = gravitational constant, 32.2 ft/sec²
g_c = force-mass conversion factor, 32.2 lbm-ft/lbf-sec²
h = static enthalpy, Btu/lbm
h_f = static enthalpy of the water in the mixed stream, Btu/lbm
h_{fg} = heat of vaporization of water at mixture temperature, Btu/lbm
h_o = total enthalpy, Btu/lbm
h_{sg} = enthalpy of saturated vapor, Btu/lbm
J = Joules constant, 778.16 ft-lbf/Btu
L = velocity ratio: velocity of water/velocity of air (after expansion)
MW = molecule weight, lbm/lb-mole
P = pressure, lbf/ft² (except where noted)
PC = propulsive coefficient, dimensionless
R = gas law constant, ft-lbf/lbm-°R
S_f = saturated water entropy at mixture temperature, Btu/lbm-°R
S_{fg} = entropy change of water by evaporation during mixing, Btu/lbm-°R
T = temperature, °R
V = velocity, fps
V_B = boat velocity, fps
V_{gg} = velocity of the exhaust from the main gas generator nozzle, fps
V_{inj} = air-water velocity ratio at the droplet injection plane
W = total mass flow rate, lbm/sec
W_B = turbofan bypass ratio
We = Weber number
X = water fraction in the water-air mixture
Z = length, coordinate in direction of flow, ft
α = water-to-air mass flow ratio in fan duct, lbm/lbm
ΔT = temperature difference between water and air after expansion, °R
λ = fractional liquid mass flow rate, lbm of liquid/lbm of mixture
ρ = density of fluid, lbm/ft³
ρ_b = mass of liquid per cubic foot of gas, lbm/ft³
σ = surface tension, lbm/sec²

Subscripts

1 = at nozzle inlet plane
2 = at nozzle exit plane
g = gas (air)
l = liquid (water)
mix = mixture

Presented as Paper 67-362 at the AIAA/SNAME Advanced Marine Vehicles Meeting, Norfolk, Va., May 22–24, 1967; submitted May 12, 1967; revision received November 6, 1967.

* Research Engineer, Systems Analysis Section.
† Senior Research Engineer, Propulsion Section.

Introduction

An increased emphasis on cruise speeds up to 100 knots[1–3] for marine surface vessels has required consideration of unconventional ship designs such as the captured air bubble, hydrofoil, and planing types. Of equal importance, however, is development of lightweight propulsion systems efficiently matched with these new designs over a wide range of speeds and having a high degree of reliability. Two such propulsion devices are the waterjet and supercavitating propeller, each driven by a lightweight, shaft-turbine engine. In many applications, however, these propulsion systems have high weights (due to the waterjet pump components and the supercavitating propeller blade and gearbox) which offset their attractive features. Lightweight, aircraft-type turbojet and turbofan engines have, therefore, been examined for high-speed marine systems; however, their characteristically high, jet exhaust velocities result in low propulsive efficiencies.

Early attempts to improve the thrust output and propulsive efficiency of aircraft-type engines by injecting water into the relatively high-temperature exhaust gas of a turbojet were unsuccessful because vaporization degraded the available energy. Similarly, water injected into the exhaust of a mixed-flow turbofan engine resulted in only a small thrust increase. Therefore, turbojet and mixed-flow turbofan engines using the momentum-exchange, water-injection concept were eliminated from consideration.

An alternative approach is to inject the water only into the fan discharge duct of a turbofan engine in which the fan and the gas generator flow streams are separated so that there is no interaction between the flows. The object of the present study was to determine what performance improvements would be attained in this manner. In theory, the transfer of momentum and energy from the fan exhaust air to the injected water should reduce exhaust velocities and increase propulsive efficiency. In addition, the water, whether containing contaminants or not, would not contact any hot engine parts (as in mixed-flow turbofans and turbojets) and, therefore, should permit extended operating periods.

Propulsion System Description

Figure 1 is a schematic diagram illustrating the use of water injection in a turbofan engine. The fan discharge duct comprises the mixing duct and the exhaust nozzle. A ram-scoop water inlet through which the injection water enters the sys-

tem is located below the hull. A duct leads from this inlet to a water manifold surrounding the engine, and appropriate water-injection nozzles extend from this manifold into the fan discharge duct. A pump could be used to inject water into the fan discharge duct, but it is not necessarily needed to attain high system propulsive efficiencies and adds mechanical complexity and weight. The characteristics of the gas generator selected for the study were those for the Pratt & Whitney JT3-type gas generator[4] with a bypass ratio of the fan of 4.0 to 1.0 and a pressure ratio of the fan of 1.5 to 1.0. It is believed, however, that the conclusions presented herein are not limited to this particular engine.

System Performance Analysis

Design-point performance studies were conducted for speeds of 25, 50, and 100 knots. The assumptions and specifications used are listed in Table 1. Net specific thrust of the engine was calculated as a function of the water-to-gas generator air mass flow ratio. Mixing calculations were based on the use of data from the gas tables[5] and steam tables.[6]

A ram pressure recovery (RPR) factor of 0.70 was used, since this value is representative of present waterjet inlet systems.[7,8] (The RPR factor is defined as the fraction of the dynamic pressure head created by the forward velocity of the vehicle and recovered in the ram-scoop water inlet.) Pressure losses due to elevation corrections were not included, since these are usually small relative to the total pressure of the inlet water and depend on vehicle design.

The velocity of fan discharge air is diffused to Mach 0.20 at the water-injection plane. It was assumed that the injected water and the fan discharge air are thoroughly and ideally mixed in the mixing duct before reaching the fan exhaust nozzle. Kinetic equilibrium was assumed within the fan exhaust nozzle, but an air-temperature drop of 10°F greater than that of the water was arbitrarily assumed.

The velocity of the mixed air-water stream at the end of the mixing duct, i.e., at the fan exhaust nozzle entrance plane, based on momentum principles, is

$$V_{\text{mix}_1} = (V_{g_1} + \alpha V_{l_1})/(1 + \alpha) \tag{1}$$

Combining the momentum and energy equations, the fraction of the injected water that is vaporized during mixing is

$$X_1 = \frac{(h_{0g} - h_{g1}) + \alpha(h_{0l} - h_{f1}) + (1/2g_cJ)\{\alpha V_l^2 - (1 + \alpha)V_{\text{mix}}^2\}}{h_{fg1}} \tag{2}$$

Also, from the relationship between the partial pressure of the air and the water

$$X_1 = [P_l/(P_{\text{mix}} - P_l)]\cdot(MW_l/MW_g) \tag{3}$$

Table 1 Assumptions and specifications used in analysis of water-injected turbofan engines

Boat speeds, knots	25, 50, and 100
Compressor pressure ratio	13.8
Compressor efficiency (polytropic), %	90
Fan bypass ratio	4.0
Fan pressure ratio	1.5
Fan efficiency (polytropic), %	90
Turbine efficiency (adiabatic), %	85
Nozzle velocity coefficient (exhaust)	0.98
Inlet air temperature, °F	60
Inlet water temperature, °F	60
Static pressure in mixing duct, psia	21.2
Water ram-scoop pressure recovery factor (RPR)	0.70
Water-to-fan air exhaust nozzle velocity ratio	1.0
Temperature difference between air and water at exit of fan exhaust nozzle, °F	10
Mixing duct drag coefficient	0

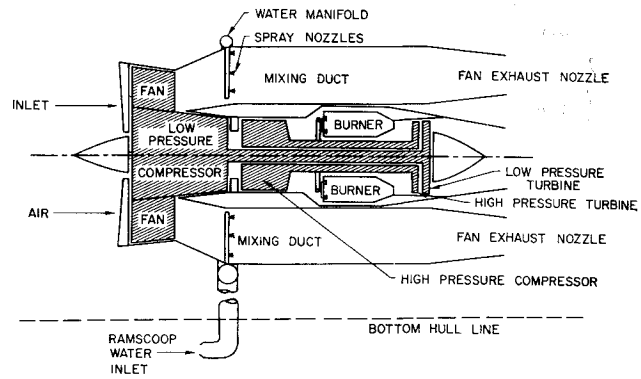

Fig. 1 Schematic of hypothetical high-bypass-ratio turbofan engine with fan duct water injection.

Solving Eqs. (2) and (3) by trial and error, with mixture temperature as the independent variable, determines the mixture water quality.

From the isentropic expansion relation for two-component flow, the fraction of the water vaporized at the fan exhaust nozzle exit plane is

$$X_2 = \frac{C_{pg}\ln\frac{T_{\text{mix}}}{T_{g_2}} - \frac{R}{J}\ln\frac{P_{\text{mix}}}{P_{g^2}} + X_1S_{fg_1} + \alpha(S_{f_1} - S_{f_2})}{S_{fg_2}} \tag{4}$$

Alternatively, this fraction can be determined from partial pressures

$$X_2 = (P_{l_2}/P_{g_2})(MW_l/MW_g)(T_{g_2}/T_{l_2}) \tag{5}$$

where the water temperature T_{l_2} is

$$T_{l_2} = T_{g_2} + \Delta T \tag{6}$$

A second trial-and-error procedure is necessary where the independent variable is air temperature at the exit plane of the fan exhaust nozzle. The extent of thermal equilibrium is controlled by selection of ΔT.

The velocity of the air-water mixture at the fan exhaust nozzle exit plane is found from a modification of the energy equation for two-component flow;

$$V_{g_2} = \{[h_{g_1} + X_1h_{sg_1} + (\alpha - X_1)h_{f_1} + \frac{[(\alpha + 1)/2g_cJ]V_{\text{mix}}^2 - h_{g_2} - X_2h_{sg_2} - (\alpha - X_2)h_{f_2}\}^{1/2}}{(1 + L^2\alpha)/2g_cJ} \tag{7}$$

Both specific thrust and system propulsive efficiency were calculated at each water-injection rate. Specific thrust is the total net thrust of the engine divided by the mass flow of the gas generator, and includes thrust losses due to the momentum drag of the inlet water and air,

$$F_{\text{net}} = \frac{W_BV_{g_2}}{g_c}(1 + \alpha L) + \frac{V_{gg}}{g_c} - \frac{V_B}{g_c}[1 + W_B(1 + \alpha)] \tag{8}$$

System propulsive efficiency is defined as the net horsepower of engine thrust divided by the gas horsepower available at the exit of the gas generator. It is slightly different from the propulsive coefficient (PC) which is the system propulsive efficiency divided by the adiabatic efficiency of the power turbine. The latter was taken to be 0.85 in this study. This difference in defining efficiencies is necessary because the water-augmented turbofan engine produces no net shaft work output. The drag due solely to locating the ram-scoop inlet outside the hull was not charged to the propulsion system, since it varies with design configuration and operating conditions and, therefore, must be considered separately in each vehicle application.

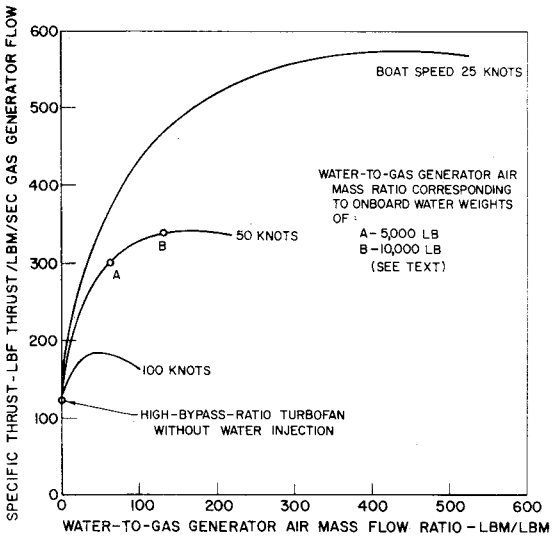

Fig. 2 Performance variation of a turbofan engine with water injection rate and boat speed. Results based on use of a Pratt & Whitney JT3-type gas generator; fan pressure ratio = 1.5:1.0; fan bypass ratio = 4.0:1.0.

Two-Phase Flow Analysis

In addition to the system performance analysis, a separate but limited analysis was performed with regard to the air-water flow behavior in the fan discharge duct. The assumptions and specifications used in the analysis are listed in Table 2. This analysis was made to estimate temperature and velocity differences between the two phases and the effect of droplet size and air-water injection velocity ratio on these differences. These are among the most important parameters that affect the net specific thrust of the propulsion system. The two-phase flow analysis indicates the representativeness of the more extensive system performance analysis in this paper.

The analysis of the air-water flow behavior in a fan discharge duct was made through a computer program that solves the differential equations for a one-dimensional, two-phase flow model. The model includes a momentum and heat balance based upon the velocity and temperature differences between the continuous gas medium and the droplets of the uniformly dispersed liquid medium. It is assumed that the total energy of the two-phase system is fixed, that the gas is nonviscous except as it exerts drag upon the particles, that heat transfer between particles and gas is by convection, that the droplets are of uniform size, and that each droplet has the same uniform temperature. The appropriate equations taken from Bailey,[9] are

Continuity

Gas

$$\rho_g V_g A = (1 - \lambda)W \tag{9}$$

Particles

$$\rho_l V_l A = \lambda W \tag{10}$$

Momentum

$$\rho_g V_g \frac{dV_g}{dZ} + \rho_l V_l \frac{dV_l}{dZ} - g_c \frac{dP}{dZ} = 0 \tag{11}$$

Energy

$$(1 - \lambda)W \left[g_c J C_{p,g} \frac{dT_g}{dZ} + V_g \frac{dV_g}{dZ} \right] + \lambda W \left[g_c J C_{p,l} \frac{dT_l}{dZ} + V_l \frac{dV_l}{dZ} \right] = 0 \tag{12}$$

State

$$P = \rho_g R_g T_g \tag{13}$$

In these equations the relative volume occupied by the droplets is assumed negligible. The effects of variable gas properties, particle drag, and heat-transfer phenomena, not restricted to Stokes flow, are included in the computer program. Not included explicitly in the computer program is droplet shattering. This condition occurs at a critical value of the Weber number, $We = \rho_g(V_g - V_l)D_p/2\sigma = 6$.[10,11] Whenever this criterion was fulfilled in a calculation, the droplet diameter was adjusted to one-fourth its original value. The assumptions that a truly dispersed flow pattern exists and that wall friction losses are negligible are based upon published experimental data under comparable flow conditions[10,12–] and are reasonable.

Discussion of Analytical Results

This section presents the theoretical design performance characteristics of the water-augmented turbofan engine at 25–100 knots, the off-design performance of the system at 5 knots, and an illustrative hydrofoil boat application. Also discussed are the performance characteristics of shaft-turbine driven waterjets and of supercavitating propellers that are used in marine vessels similar to those considered for the water augmented turbofan engine. Comparative performance levels and weights for shaft-turbine-driven waterjets and supercavitating marine propellers are based on published data.[15,16] The effect of air-water flow behavior on theoretical design performance characteristics, as determined in the two-phase flow analysis, is also discussed.

Engine Design-Point Performance

The theoretical design-point specific thrust of the water augmented turbofan engine is shown in Fig. 2 as a function of water-to-gas generator air mass flow ratio and boat speed. Maximum values of specific thrust are 576, 341, and 192 lb thrust/lbm/sec of gas generator air for vehicle speeds of 25, 50 and 100 knots, respectively. These values compare with the dry engine specific thrust ratings of 121, 118, and 106 lb thrust/lbm/sec of gas generator air, respectively. As the water-to-gas generator air mass flow ratio is increased, the augmented thrust due to increased mass flow predominates over the associated inlet water momentum drag until a maximum value of thrust is reached. At higher values of this ratio, the momentum drag of inlet water predominates. The high levels of thrust in this system can be partially attributed to the fact that little (less than 1%) of the injected water is vaporized in the relatively cool (approximately 160°F) fan air stream, in contrast to the situation in water-augmented turbojects and mixed-flow turbofan engines. The exhaust flow, therefore, consists primarily of liquid water droplets and air. The fluid dynamic behavior of this two-phase flow is similar to that experimentally observed in the studies reported by Elliott.[10]

Table 2 Assumptions and specifications used in two phase flow analysis

Boat speed, knots	50
Inlet air temperature, °F	130
Inlet water temperature, °F	60
Air velocity at droplet injection plane, fps	119
Water-gas generator air mass flow ratio	80
Water-fan air mass flow ratio	20
Mass flow rate of gas generator air, lbm/sec	188
Flow area of fan discharge duct at droplet injection plane, ft²	62.
Length of mixing duct, ft	9.
Convergent half-angle of exhaust nozzle, deg	30

The results in Fig. 2 indicate that relatively large water flow rates are necessary to attain maximum system performance. For example, at 25 knots the water flow rate necessary to attain the maximum theoretical specific thrust of 576 lbf/lbm/sec of gas generator airflow exceeds 80,000 lbm/sec, and the onboard water weight (within the engine and inlet ducts) exceeds 45,000 lbm. This extremely large onboard water weight would, in all likelihood, preclude operation near the point of maximum thrust and is a major consideration for operation at speeds below 50 knots.

The theoretical system propulsive efficiencies corresponding to the points of maximum specific thrust are shown in Fig. 3 as a function of boat speed. System propulsive efficiency is considerably better than that of the same turbofan without water augmentation. Maximum theoretical system propulsive efficiency is over 42% at 50 knots and over 46% at 100 knots.

Off-Design Performance

Since the water inlet duct would most likely be a fixed-geometry design sized for a particular boat speed, performance compromises will have to be made to operate the water-injected turbofan engine over a range of boat speeds. For example, the propulsion system duct areas may be designed to handle water flow rates less than those corresponding to maximum attainable specific thrust at a given speed. In this case, the engine performance would be lowered, but the weight of onboard water would be decreased significantly. Two examples (points A and B in Fig. 2), illustrating specific compromises between engine performance and onboard water weight, are shown along with the curve of maximum thrust in Fig. 4. Each of the two curves corresponds to the performance of a single engine system with variable exhaust nozzles and fixed-geometry water inlet and mixing ducts. These two systems have 10-ft-long inlet water ducts, ram-scoop capture areas of 4.5 and 9.1 ft^2, and total onboard water weights of 5000 and 10,000 lbm (at a 50 knot design speed), respectively. Although the amounts of water within a system with fixed-geometry inlet water and mixing ducts may vary somewhat with speed, these slight variations of total onboard water weight are of minor importance. The water-handling capability of each system was based on a ram-scoop capture area ratio of 1.0, and at all speeds no variations were considered in engine aerodynamic design or operation. In addition, the water flow rate was assumed to vary with boat speed, and no regulating devices were assumed to reduce onboard water weight during reduced-speed operation.

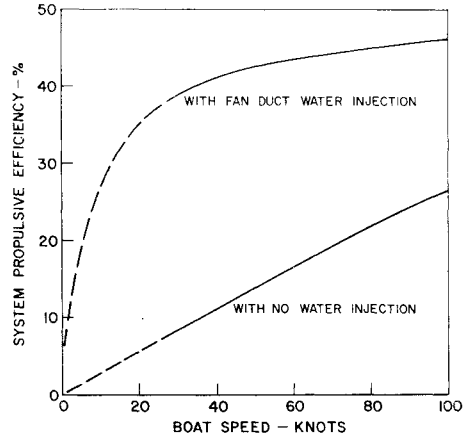

Fig. 3 System propulsive efficiencies of a high-bypass-ratio turbofan engine. Calculations based on use of a Pratt & Whitney JT3-type gas generator; fan bypass ratio 4.0:1.0; fan pressure ratio = 1.5:1.0; system propulsive efficiency = propulsive coefficient × power turbine efficiency.

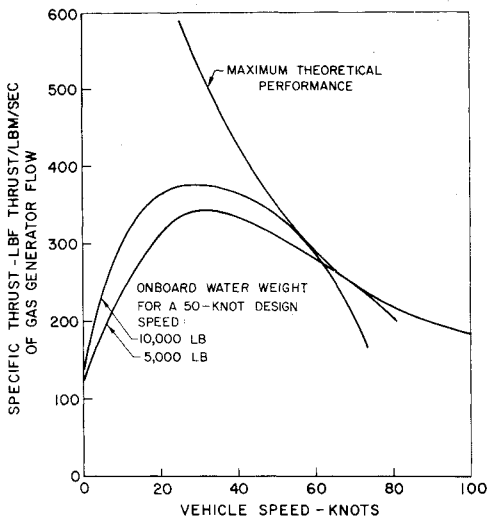

Fig. 4 Off-design performance of water-augmented turbofan engines. Fan bypass ratio = 4.0:1.0; fan pressure ratio = 1.5:1.0; JT3-type gas generator engines include variable exhaust nozzles; inlet water duct length = 10 ft.

At a fixed vehicle speed, the weight of onboard water increases with water injection rate much more rapidly than does the specific thrust. For example, at 25 knots the theoretical specific thrust of a system that is sized (at 50 knots) to accommodate only 5000 lbm of onboard water is 335 lbf/lbm/sec, while the specific thrust of an engine with ducts sized to accommodate 10,000 lbm of onboard water is 375 lbf/lbm/sec. This corresponds to a performance improvement of approximately 12% for a 100% increase in water weight. Notwithstanding the compromises that must be made with maximum theoretical performance, the results indicate that sizable thrust augmentation levels can be realized over the entire vehicle speed range.

Performance Variation with Bypass Ratio

Associated studies have shown that the performance of the water-augmented turbofan increases considerably with bypass ratio. This is shown in Fig. 5 for maximum theoretical specific thrust vs turbofan bypass ratio at a boat speed of 50 knots. The increase in specific thrust is due not only to water injection, but also to the increase in dry thrust with bypass ratio, as shown by the lower curve. The results given in Fig. 5 were calculated for engines with a JT3-type gas generator as described previously.

Vehicle Applications

A smooth-water hydrodynamic drag curve and a turbofan installed thrust curve are shown in Fig. 6 for a 76-ton hydro-

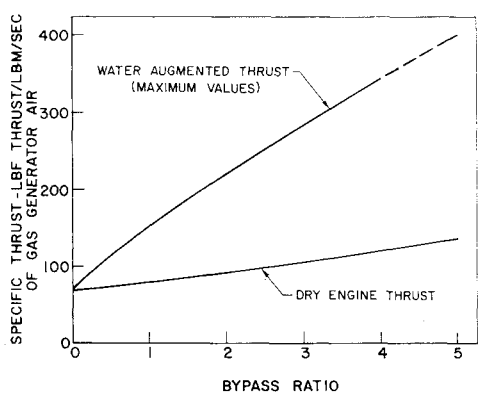

Fig. 5 Maximum specific thrust at various bypass ratios with a JT3-type gas generator. Boat speed = 50 knots.

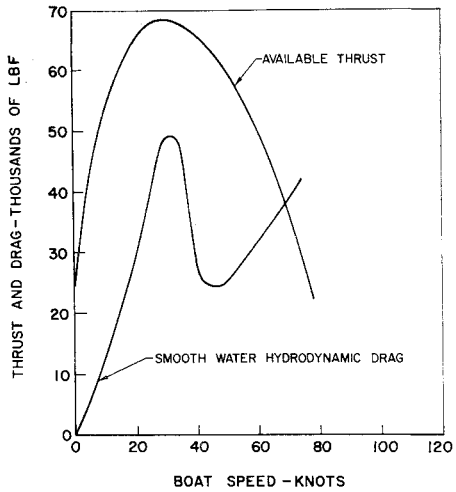

Fig. 6 Hypothetical hydrofoil boat drag and water-augmented turbofan installed thrust. Onboard water weight = 10,000 lb; hydrofoil boat displacement = 76 tons; turbofan uses JT3-type gas generator.

foil ship. The available thrust curve corresponds to the estimated total thrust output of water-augmented turbofan engine with 10,000 lbm of onboard water, based on data from Fig. 4, and the results of the two-phase flow analysis presented below. The hydrodynamic drag curve for the hypothetical hydrofoil ship is from Gill.[17] The intersection of the thrust and drag curves indicates that this ship should be capable of attaining a maximum smooth-water speed of approximately 69 knots. A 40% margin of available thrust-to-vehicle drag was assumed at take-off to allow for sea-state conditions.

The performance of a waterjet propulsion system installed in the hydrofoil ship with the drag curve of Fig. 6 was also estimated in order to compare it with the water-augmented turbofan engine. The design thrust of the waterjet system at 69 knots was specified to be the same as that of the water-augmented turbofan. The waterjet pump is estimated to weigh 8400 lbm, the shaft-turbine engine 11,800 lbm, the water within the pump and its ducts 20,000 lbm (essentially double that dry system component weights), and the total system 42,220 lbm.[18,19] By comparison, the dry weight of the water-augmented turbofan engine is estimated to be approximately 9800 lb and the total system weight approximately 19,800 lbm. Weight breakdowns are shown in Table 3. The payload fraction and range characteristics of the 76-ton hydrofoil ship propelled at a cruise speed of 69 knots by a water-augmented

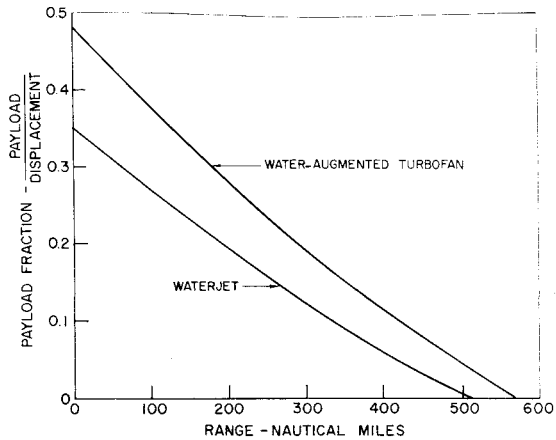

Fig. 7 Payload capability of hydrofoil ships. Displacement = 76 tons; cruise speed = 69 knots; onboard water weight for turbofan is 10,000 lb, for waterjet is 20,000 lb; 36% propulsive efficiency for turbofan, 50% for waterjet; hydrofoil drag shown in Fig. 6.

Table 3 Estimated water-augmented turbofan and waterjet weights

Wate -augmented turbofan

Component	Weight, lb
JT3-type gas generator	4,200
Power turbine (4 stages)	1,866
Fan (4.0–1.0 bypass ratio, 1.5–1.0 pressure ratio)	795
Fan mixing duct (13-ft-long, stainless steel)	1,470[a]
Water inlet duct (10-ft-long, stainless st el)	360[a]
Spray nozzles	200
Subtotal	8,891
Supports, etc. (10% of subtotal weight)	889
Total dry system weight	9,780
System weight with onboard water weight of:	
2500 lb	12,280
5000 lb	14,780
10,000 lb	19,780

Gas-turbine-driven waterjet

Component	Weight, lb
FT3-turbine drive	11,800
Waterjet (dry)	8,400
Subtotal	20,200
Supports, etc. (10% of subtotal weight)	2,020
Total dry system weight	22,220
Weight of system with onboard water (20,000 lb)	42,220

[a] For ⅛-in-thick sheet.

turbofan engine or by a waterjet driven by a shaft turbi engine are shown in Fig. 7. The system propulsive e ficiencies of the water-augmented turbofan and waterjet we estimated at 36 and 50%, respectively. The payload fracti for the waterjet-propelled hydrofoil ship never equals that the ship propelled with the water-augmented turbofan engi In this example, the increased weight of the waterjet syste more than offsets its higher propulsive efficiency. Althou the hydrofoil ship selected is relatively small, a similar a vantage is shown when multiple units of the water-augment turbofan engine are compared with waterjets driven by sha turbine engines in larger hydrofoil ships. The total machine weight of a gas-turbine-driven, supercavitating, marine pr peller system capable of propelling the same 76-ton hydrof ship is estimated to be over 40,000 lb, based on a gear-b weight of 2 lbm/hp,[16] which is optimistic for the rather seve service and required extended lifetime of a hydrofoil shi

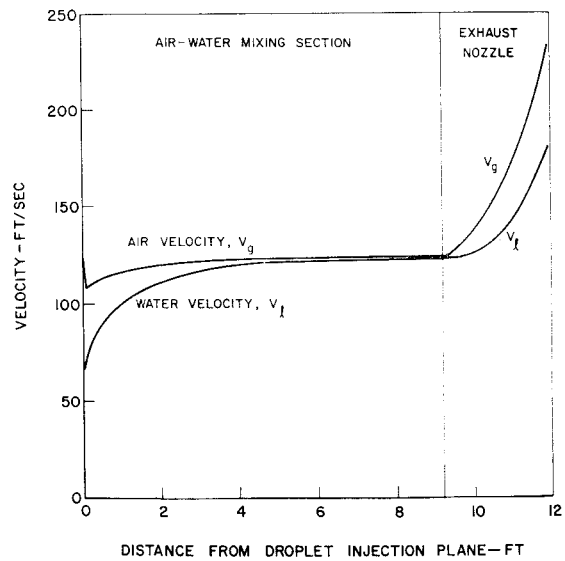

Fig. 8 Axial velocity profiles of gas and liquid phases fan discharge duct; D_{po} = 100μ; V_{inj} = 2; boat speed 50 knots.

Although model tank tests indicate that a *PC* of 0.70 to 0.75 can be attained by supercavitating propellers, installed *PC* probably will be no greater than 0.65, corresponding to a system propulsive efficiency of approximately 0.55. The payload fraction for this system is close to that of the waterjet, but still far below that of the water-augmented turbofan installed in the 76-ton ship.

Results of Two-Phase Flow Analysis

The results of a typical two-phase flow example calculation are shown in Fig. 8, where axial velocity profiles of the two phases in the fan discharge duct are shown as a function of duct length for 100-μ-diam droplets. No droplet shattering took place, and both thermal and dynamic equilibria between the two phases are essentially achieved before the exhaust nozzle. By contrast, for droplets with initial diameters greater than 400 μ, droplet shattering was normally achieved, and for droplets with initial diameters greater than approximately 250 μ dynamic equilibrium was not normally achieved. Nozzle discharge velocities of each phase are shown in Fig. 9 as a function of initial droplet diameter D_{po} and the air-water velocity ratio at the droplet injection plane, V_{inj}. Net specific thrust is presented in Fig. 10.

The results of the two-phase flow calculations indicate 1) that the effect on performance of the air-water injection velocity ratio is increased at low droplet diameters (less than approximately 100 μ), and 2) that the effect of droplet diameter on performance is negligible, because of droplet shattering, for initial droplet diameters greater than approximately 400 μ. For a 50-knot ship the available pressure head will not allow the value of V_{inj} to be much less than 2.0, and droplet diameters much less than 400 μ can then be achieved only with orifices of very small diameter. Such orifices permit low flow rates, and a prohibitively large number might be required to provide the total liquid flow rate. On the other hand, spray nozzles with large flow rate, which produce droplets with mean diameters greater than 1000 μ, reduce system performance only slightly, relative to the performance provided by 400-μ droplets. This relaxes the actual design constraints for the liquid spray nozzles. The predicted net specific thrust of the water-augmented turbofan engine, therefore, may be as much as 100% greater than that of a dry turbofan engine at a boat speed of 50 knots.

Concluding Remarks

The system performance analysis shows that the thrust of a water-augmented, high-bypass-ratio turbofan with separate fan and gas generator exhaust nozzles theoretically can be increased by amounts varying from 380% at 25 knots to 90% at 100 knots, relative to the thrust of this engine without water injection. Although the rate of water that must be injected is considerable at the points of maximum thrust, lower water-injection rates still provide sizable thrust augmentation at all boat speeds.

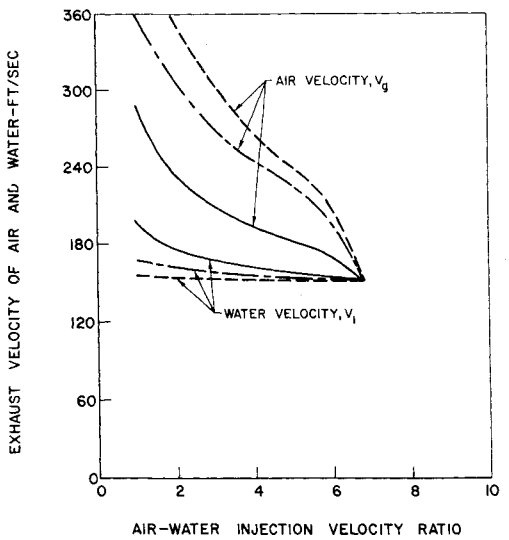

Fig. 9 Velocities of air and water phases leaving exhaust nozzle of fan discharge duct. Air velocity at injection plane = 119 fps; D_{po}, μ; —— 100; — - — 500; --- 1000.

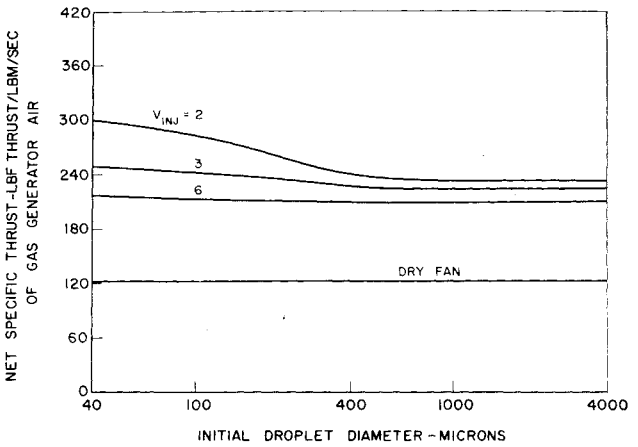

Fig. 10 Performance of water-augmented turbofan engine. Design conditions specified in Tables 1 and 3; boat speed = 50 knots.

Low system weight and good performance made the water-augmented turbofan competitive with the waterjets and supercavitating marine propellers driven by shaft-turbine engines, particularly in the hydrofoil and planing boats.

The system performance analysis and two-phase flow calculations utilized in this paper are in close agreement when the dispersed water phase consists of droplets with diameters less than 40 μ. At larger diameters, the two-phase flow calculations indicate lower values of thrust augmentation, because of frictional and acceleration effects between the two phases. However, because of droplet shattering effects, performance values become relatively insensitive to droplet diameter initially greater than 400 μ. To realize the full potential of the concept of the water-augmented turbofan, attention must be directed toward the injection scheme; however, a relatively small performance penalty occurs with large-capacity state-of-the-art spray nozzles.

An advantage of the water-augmented turbofan system not previously mentioned is that of a low-draft system with only the water ram-scoop inlet protruding below the hull line. In addition, reduced propulsive thrust is still available if the primary ram-scoop inlet areas become congested. The "unaugmented" thrust may be beneficial to landing craft that move beyond the beach area. Further, occasional air ingestion through the water ram-scoop will not unload the turbine and thereby cause shock loading on the pump and drive shaft parts, as might occur in a waterjet when air flows through the ducting.

References

[1] Chaplin, H. A. and Ford, A. G., "Some Design Principles Ground Effect Machines, Section A—Introductory Survey Rept. 2121A, April 1966, David Taylor Model Basin.

[2] Meyers, G. R., "Observations and Comments on Hydrofoils," Paper 2a, May 13–14, 1965, Society of Naval Architects and Marine Engineers, Seattle, Wash.

[3] Savitski, D., "Hydrodynamic Design of Planing Hull Rept. 1000, Davidson Lab., Stevens Institute of Technology.

[4] *Military Turbofan Installation Handbook, JT3D Engi* April 1959, Pratt & Whitney Aircraft, East Hartford, Conn.

[5] Keenan, J. H. and Kay, J., *Gas Tables*, Wiley, New Yo 1956.

[6] Keenan, J. H. and Keyes, F. G., *Thermodynamic Properties Steam*, Wiley, New York, 1950.

[7] Engel, W. N., Cochran, R. L., and Delao, M. M., "Use of Axial Flow Pumps for Marine Propulsion," Paper 442A, January 8–12, 1962, Society of Automotive Engineers, Detroit, Mich.

[8] Gongwer, C. A., "The Influence of Duct Losses on Jet Propulsion Devices," *Jet Propulsion*, Vol. 24, Nov.-Dec. 1954, pp. 385–386.

[9] Bailey, W. S. et al., "Gas-Particle Flow in an Axisymmetric Nozzle," *ARS Journal*, Vol. 31, June 1961, pp. 793–798.

[10] Elliott, D. G., "Analysis of the Acceleration of Lithium in a Two-Phase Nozzle," *Proceedings of 1963 High-Temperature Liquid Metal Heat Transfer Technology Meeting*, Oak Ridge, Tenn., Dec. 1964.

[11] Lane, W. R. and Green, H. L., "The Mechanics of Drops and Bubbles," *Surveys in Mechanics*, Cambridge University, London, 1956, pp. 162–215.

[12] Scott, D. S., "Properties of Concurrent Gas-Liquid Flow," *Advances in Chemical Engineering*, Vol. 4, Academic Press, New York, 1963, pp. 200–278.

[13] Martinelli, R. D. and Nelson, D. B., "Prediction of Pressure Drop During Forced Circulation Boiling of Water," *Transactions of the American Society of Mechanical Engineers*, Vol. 70, A 1948, pp. 695–702.

[14] Vance, W. H. and Moulton, R. W., "A Study of Slip Rat for the Flow of Steam-Water Mixtures at High Void Fraction *American Institute of Chemical Engineers Journal*, Vol. 11, N 1965, pp. 1114–1124.

[15] Arcand, L., "Waterjet Propulsion for Small Craft," Pa F, Southwest Section Meeting, May 26–28, 1966, Society Naval Architects and Marine Engineers, Miami, Fla.

[16] Tulen, M. P., "Supercavitating Propellers—History, Oper ing Characteristics, and Mechanism of Operation," *Proceedi of Fourth ONR Symposium on Naval Hydrodynamics*, 19 Washington, D. C.

[17] Gill, J. D., "The Hydrofoil Commuter," *Boat Construct and Maintenance*, Feb. 1965.

[18] "Fact Sheet, FT3C-9 Marine Gas Turbine," May 17, 19 Pratt & Whitney Aircraft, East Hartford, Conn.

[19] "A Parametric Study of Hydrofoil Ships," U.S. Na Bureau of Ships Rept. D2-20671-3, Dec. 1963, The Boeing C Seattle, Wash.

JANUARY 1968 J. HYDRONAUTICS VOL. 2, NO

Selection and Utilization of Batteries for Deep Submergence Vehicles

N. KUSKA* AND J. A. CRONANDER†
North American Rockwell Corporation, Long Beach, Calif.

A brief review of battery characteristics is presented. The mission parameters of a deep submergence vehicle that affect battery cell selection are mentioned, as well as a few of the pitfalls and problem areas which can be encountered. The conception and design of a battery container system is discussed, including electrolyte reservoirs, pressure compensators and gas vent valves. The results of a battery system test program are covered including capacity, charging, gassing, and significant findings.

Introduction

As dive depths of submersible vehicles increased, ways to reduce weight or increase buoyancy became paramount. This led to power system storage batteries external to the pressure hull. In this location, they could be operated at ambient sea pressure, wherein a savings in volume and weight could be realized. Problems of temperature control and ventilation became ones of pressure compensation, insulation, and material compatibility, with a few added ones of maintenance, control, and reliability.

Characteristics of Candidate Cells

Table 1 presents some characteristics of candidate cell types. Lead-acid cells have been used on most deep submergence vehicles where the batteries are located external to the pressure hull. Except when low-energy density rules out the lead-acid battery, it will probably see extensive use for a long time to come. It is a proven, inexpensive, rugged, reliable, and relatively easy-to-service source of power. It also has a high cell voltage, relatively long cycle life, and trou free service life. There are no off-the-shelf units desig specifically for use external to the pressure hull. All insta tions have been adaptations of automobile, truck, golf cart, industrial cells. This has resulted in larger, heavier, and, some cases, shorter lived installations than could be obtai from cells especially designed for the ocean environment.

Silver-zinc cells are currently being developed for d submersible use in the ocean environment. This cell typ characterized by its high energy density, tolerance to h rates of discharge, and long dry-storage life. Its dis vantages are high cost, short cycle life for deep discha cycles, short wet-storage life, and difficulty in determin state of charge.

The silver-cadmium cell combines the high energy dens of the silver anode with the long life of the cadmium catho As was shown in Table 1, the energy density is somewhat l than that of silver-zinc, but the increased cycle life may ov come this for some applications. Cost per cell is close to t of silver-zinc, but more cells are required because the nomi cell voltage is lower. The silver-cadmium battery can charged fast and has a long dry-storage life.

Mission

Factors in a deep submersible mission which can aff battery selection are dive depth, energy requirements, sponse time, standby requirements, and permissible ma

Presented as Paper 67-368 at the AIAA/SNAME Advance Marine Vehicles Meeting, Norfolk, Va., May 22–24, 1967; submitted May 22, 1967; revision received September 27, 1967.

* Chief, Subsystems and Components, Ocean Systems Operations.

† Member, Technical Staff, Ocean Systems Operations.